

# Airflow Measurement of the Car HVAC Unit Using Hot-wire Anemometry

Miloš Fojtlin<sup>1,a</sup>, Michal Planka<sup>1</sup>, Jan Fišer<sup>1</sup>, Jan Pokorný<sup>1</sup> and Miroslav Jicha<sup>1</sup>

<sup>1</sup>*Department of Thermodynamics and Environmental Engineering, Energy Institute, Faculty of mechanical engineering, Brno University of Technology, Czech Republic.*

**Abstract.** Thermal environment in a vehicular cabin significantly influence drivers' fatigue and passengers' thermal comfort. This environment is traditionally managed by HVAC cabin system that distributes air and modifies its properties. In order to simulate cabin thermal behaviour, amount of the air led through car vents must be determined. The aim of this study was to develop methodology to measure airflow from the vents, and consequently calculate corresponding air distribution coefficients. Three climatic cases were selected to match European winter, summer, and spring / fall conditions. Experiments were conducted on a test vehicle in a climatic chamber. The car HVAC system was set to automatic control mode, and the measurements were executed after the system stabilisation—each case was independently measured three times. To be able to evaluate precision of the method, the airflow was determined at the system inlet (HVAC suction) and outlet (each vent), and the total airflow values were compared. The airflow was calculated by determining a mean value of the air velocity multiplied by an area of inlet / outlet cross-section. Hot-wire anemometry was involved to measure the air velocity. Regarding the summer case, total airflow entering the cabin was around  $57 \text{ l s}^{-1}$  with 60 % of the air entering the cabin through dashboard vents; no air was supplied to the feet compartment. The remaining cases had the same total airflow of around  $42 \text{ l s}^{-1}$ , and the air distribution was focused mainly on feet and windows. The inlet and outlet airflow values show a good match with a maximum mass differential of 8.3 %.

## 1 Introduction

Europeans spend significant amount of time indoors in buildings and vehicles [1]. Consequently, proper indoor microclimate in relation to air quality, thermal comfort and other factors is important [2]. Regarding vehicular microclimate, inappropriate thermal environment has also a negative impact on drivers' fatigue and focus. Traditionally, microclimate in vehicles is managed via HVAC (Heating Ventilation and Air-conditioning) system. Besides others, the HVAC system also provides defogging or defrosting of windscreens, thus creating conditions for safer driving. These all HVAC features are achieved through smart distribution of the air with an appropriate air speed, temperature and humidity.

This work will analyse the air distribution within a passenger vehicle cabin with a focus on airflow through HVAC vents and calculation of corresponding air distribution coefficients. The HVAC will be set to automatic control mode and three interior temperatures will be studied. Both, system inlet and outlet airflow will be monitored to compare a match of these two values. The aim of this study is to develop a methodology to measure the airflow simply and relatively precisely. Next, three cases will be examined to match central European winter, summer and spring/fall ambient conditions. The

experiments will be conducted in a laboratory of thermal comfort at the University of Technology Brno inside a climate chamber. Outcomes of this study will serve also as a reliable source of boundary conditions to numerical simulations of a car cabin.

## 2 Methods

To develop a simple and efficient methodology to measure airflow from the vents we needed to measure the airflow entering the HVAC system precisely. Thus, we were able to compare “the input” with the airflow leaving the vents in the car cabin. The vents were measured with a less precise and less time consuming method. Match of these two parameters was then studied.

### 2.1 HVAC system description

Nowadays, the HVAC systems in passenger vehicles are conceptually very similar. Firstly, fresh air is supplied from a front grille located below a windshield and the air is let through filters. Amount of the supplied fresh air is adjusted by an air recirculation door. Next, the airflow is driven by a centrifugal fan, the air passes heat exchangers and final air temperature is achieved in a mixing

<sup>a</sup>Corresponding author: [milos.fojtlin@vut.cz](mailto:milos.fojtlin@vut.cz)

chamber. Now, the air is ready to be introduced to the cabin via air ducts and vents (Figure 1. and 2.). The whole process is controlled manually or by an HVAC control unit, when an automatic control mode is used. This study involved the automatic control mode that selects optimal settings based on ambient temperature, intensity of solar radiation and other numerous factors. Finally, the air leaves the cabin through openings with flaps mounted under a rear bumper.

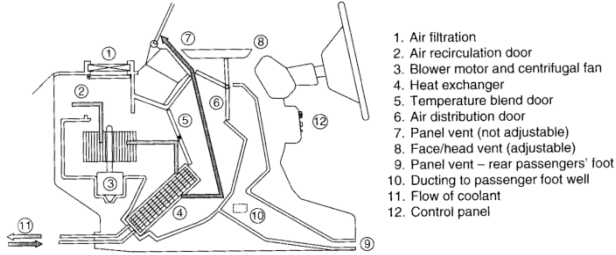


**Figure 1.** Schematic design of the vehicular HVAC system [3].

The test car possesses one inlet opening and 25 various vents in the interior. Vents arrangement of the test car shows Figure 2, complete description, surface area, and number of measurement points are shown in Table 1.

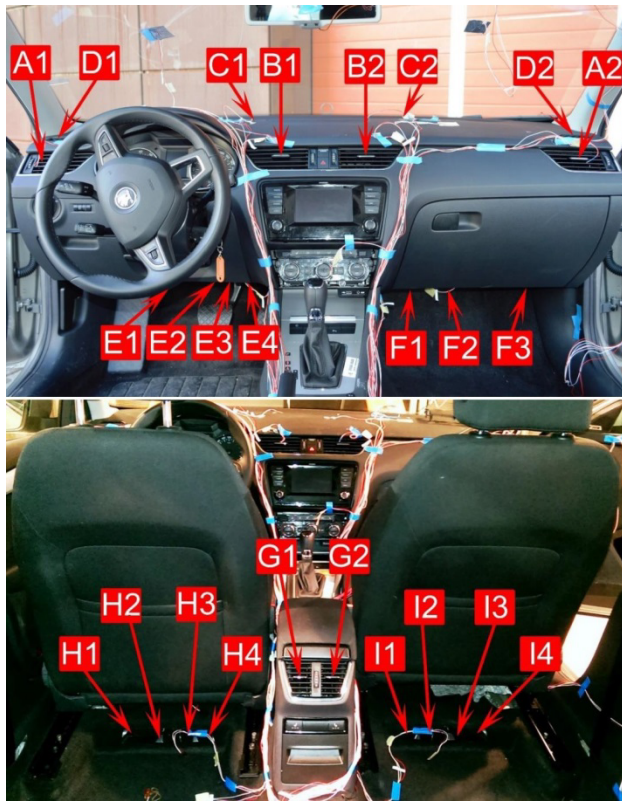


**Figure 2.** Arrangement of the vents in the tested vehicle.

Some of the vents are equipped with directional flaps and butterfly valves to adjust the flow direction and amount of the supplied air. During the experiments, all of the vents were fully opened and set to a neutral position. Next, it was found that an air pressure fluctuates inside the cabin when the cabin is closed. We ascribed this phenomenon to a cyclic opening and closing of the outlet

flaps. Stability of the airflow entering the cabin and the measurement reproducibility was thus negatively influenced. Therefore, a trunk of the car was ajar. This helped to eliminate the fluctuations.

**Table 1.** Vents description, surface area, number of local air speed measurement points and proportional coefficients.

tag	description	S (cm <sup>2</sup> )	no. of $w_i$	$k_m$
A1	L dashb.	50.4	4	0.58
A2	R dashb.	50.4	4	0.58
B1	L centr. dashb.	66.8	4	0.57
B2	R centr. dashb.	66.8	4	0.57
C1	L defrost	42.0	3	0.91
C2	R defrost	42.0	3	0.91
D1	L window	18.6	1	0.84
D2	R window	18.6	1	0.84
E1-4	L Feet fr.	11.3; 3.8; 4.3; 5.1	$4 \times 1$	1
F1,2,3	R feet fr.	18.2; 17.8; 12.9	$3 \times 1$	1
G1	L centr. bk.	26.9	2	0.65
G2	R centr. bk.	26.9	2	0.65
H1-4	L feet bk	20.0; 9.8; 7.0; 12.6	$4 \times 1$	1
I1-4	R feet bk	12.6; 7.0; 9.8; 20.0	$4 \times 1$	1

## 2.2 Airflow measurement

Hotwire anemometry was used to measure local air speeds  $w_i$  at the system inlet (suction) and outlet (vents). Mean airspeed  $\bar{w}$  was calculated using averaging method. The experiment was designed that  $w_i$  measurement points were evenly distributed across the examined area and each point represented the same area fraction. Thus,  $\bar{w}$  is defined as the arithmetic mean of  $w_i$ . Number of measurement points per vent shows Table 1. For circular cross-section with radius  $R$ ,  $w_i$  is determined at pre-calculated radial distances from the center point  $r_i$  using formula (1) – equidistant spacing using a transformed coordinate ( $r/R$ ) in an interval from 0 to 1 [4],

$$r_i = R \sqrt{\frac{2i-1}{2n}} \quad (1)$$

where  $n$  is the number of measurement points;  $i$  is the sequence number of the measurement point from 1<sup>st</sup> to  $n^{\text{th}}$ . Next, to calculate airflow  $q$  formula (2) was applied

$$q = \bar{w} S k_m \quad (2)$$

where  $\bar{w}$  is the corresponding mean air speed,  $\text{m s}^{-1}$ ;  $S$  is the cross section of the vent or the inlet piping,  $\text{m}^2$ ;  $k_m$  is a proportional coefficient to compensate solid cross-section area of the vents if there are the directional flaps present (Table 1). Mass flow of the air  $q_m$  was defined as

$$q_m = q \rho \quad (3)$$

where  $\rho$  is the air,  $\text{kg m}^{-3}$ . Since low air humidity (up to 20 %) was present during the test, modified equation of state was used

$$\rho = \frac{p}{rT} \quad (4)$$

where  $p$  is the air pressure, Pa (100 kPa was used);  $r$  is a specific gas constant of a dry air,  $\text{J kg}^{-1} \text{K}^{-1}$ ;  $T$  is temperature, K.



### 2.2.1 Airflow at the HVAC system inlet

To determine the airflow at the inlet was a challenging task because of following conditions: 1. difficult access to the actual opening; 2. influence of the measurements due to blowing air from the engine fans; 3. unpredictable behavior of recirculation door that influences amount of fresh air entering the cabin.

Firstly, the car hood was disassembled and plastic covers of the suction were removed. Secondly, after several unsuccessful attempts to determine the inlet airflow by a handheld anemometric probe, we decided to mount an inlet tube with an adapter instead of the original grille (Figure 3. and 4.). The tube was 2 m long with diameter of 150 mm. Cross-section area of the tube and the grille was the same. It was also assumed that pressure losses in the tube are similar to the pressure losses induced by the grille, and the measurements are not significantly influenced by this substitution. Thirdly, the recirculation door was kept open to be able to compare the inlet and outlet airflow.



**Figure 3.** Positioning and shape of the inlet grille; the first attempts to measure the inlet airflow directly without the tube.



**Figure 4.** The suction tube with the adapter – a final assembly.

Omnidirectional anemometric and temperature probe Testo 350 M/XL-454 was used to examine airspeed in the

tube. The local airspeed was determined in the middle of the tube length (that is 6.6 tube diameters) corresponding to Figure 5. It was also expected that the tube stabilizes the flow contributing to improve measurement precision. Each point was measured 10 times independently for each of the cases. Local airspeed of one point yielded from 2 s measurement average. At the same time, voltage of the HVAC fan was monitored. It was assumed that the fan voltage corresponds to the airflow and can serve as rough airflow estimation.

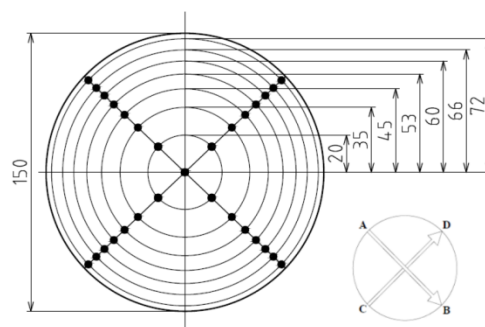


**Figure 5.** Pre-calculated points of  $w_i$  measurement according to the formula (1); quarters of measurement A-B, C-D.

### 2.2.2 Airflow at the HVAC system outlet

Airspeed was measured circa 2 cm in front of the vents at specified points by a handheld combined probe (airspeed, temperature and humidity) with a logger Testo 435. Number of the points varied due to diversity of vent shapes and final number of the measurement points per vent is indicated in Table 1. However, other methods to determine the airflow were considered, but as it could be

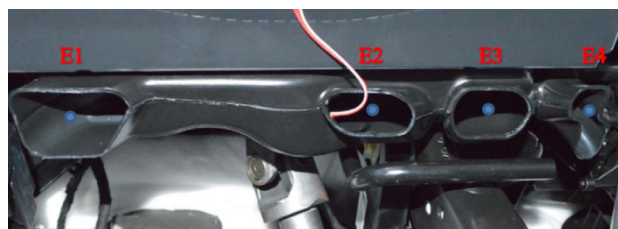


**Figure 6.** Example – points of  $w_i$  measurement at the vent A1 (upper picture) and vents E1-4 located in the foot well.

seen in Figure 6., the vents pointing to the foot well are hardly accessible and have an irregular shape. This excludes most of the conventional airflow measurement methods.

The local airspeed was determined from 10 s average, and measurement in each point was repeated three times a case.

### 2.3 Experimental procedure

Firstly, the experimental vehicle was placed inside the climate chamber. Next, the climate chamber and the artificial solar system were initiated to reach desired ambient conditions, details presents Table 2. Typically, the preconditioning of the chamber with the car inside lasted one hour. Then, the vehicle was started up and the automatic HVAC system was set to desired interior temperature. The actual measurements started after around 45 minutes when the automatic control mode reached stable thermal conditions within the cabin.

**Table 2.** Boundary conditions of the experiment

case	$t_{\text{set}} (^{\circ}\text{C})$	$t_{\text{chamber}} (^{\circ}\text{C})$	$I_{\text{solar}} (\text{W m}^{-2})$
summer	auto 23	30	800
spring / fall	auto 22	16	400
winter	auto 18	-2	0

Measurements were performed by two operators, one determining airflow through vents in the car, and the other examining the inlet airflow to the HVAC system outside. Performance of each case lasted around 40 min.

### 2.4 Statistical data evaluation

As long as no measurement is perfectly precise, there is a need to express uncertainty of the estimated value (measurement). This study dealt with the type A and B uncertainty evaluation of the airflow and the mass flow. Next, we adopted presumption that uncertainty of the air density calculation and the cross-section measurement had a small impact on the results. However, the main focus was on the airspeed uncertainty evaluation.

Type A uncertainty is represented by a statistically estimated sample standard deviation of the mean  $u_A(x)$  (5) [5,6,7]. Formula (5) is valid under following conditions: 1. variable  $x$  follows a normal probability distribution; 2. the data origin from independent observations performed under the same conditions. Our previous experience proves normal probability distribution of the data.

$$u_A(x) = k_{uA} \left[ \frac{1}{n(n-1)} \sum_{i=1}^n (x_i - \bar{x})^2 \right]^{\frac{1}{2}} \quad (5)$$

where  $u_A(x)$  is the type A uncertainty of the variable  $x$ ;  $n$  is the number of the independent observations;  $x_i$  is the value of the  $i^{\text{th}}$  variable  $x$ ;  $\bar{x}$  is the mean value of  $x$ ;  $k_{uA}$  is the safety factor.

This study dealt with 10 observations in the case of the inlet measurements, thus safety factor  $k_{uA} = 1$ . Regarding the vents,  $k_{uA} = 2.3$  was applied to compensate missing data because of the three observations a case [8].

The type B uncertainty  $u_B(x)$  is an evaluation method by means other than the statistical data evaluation. We considered only the uncertainty due to limited precision of the anemometers (Table 3). Other sources of the B type uncertainty were omitted.

Next, expanded combined uncertainty was expressed as follows

$$U = k u = k \sqrt{u_A(x)^2 + u_B(x)^2} \quad (6)$$

where  $k$  is the coverage factor,  $k = 2$  was applied to achieve 95 % level of confidence;  $u$  is the combined uncertainty (confidence level ca 68.3 %).

**Table 3.** Precision of the anemometers

anemometer	precision	note
Testo 350M/XL	$\pm 0.02 \text{ m}\cdot\text{s}^{-1}$	inlet
Testo 435	$\pm 0.02 \text{ m}\cdot\text{s}^{-1} + 4 \% \text{ of est. value}$	outlet

Uncertainty of an indirect independent measurement is a function of each uncertainty from which the final uncertainty is calculated. If the final quantity  $x$  is a function of quantities  $a, b, c, \dots$ , the final uncertainty  $u_x$  is calculated as follows [8]

$$x = f(a, b, c \dots) \quad (7)$$

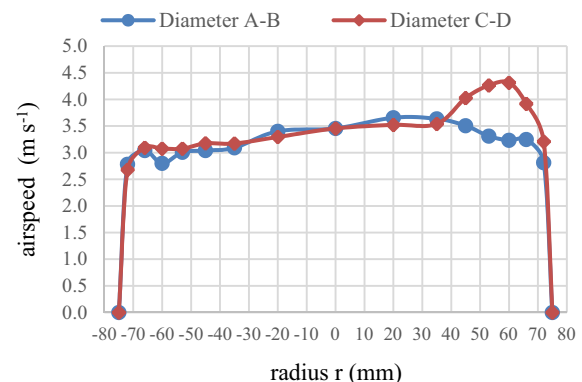
$$u_x = \sqrt{\left(\frac{\partial f}{\partial a} u_a\right)^2 + \left(\frac{\partial f}{\partial b} u_b\right)^2 + \left(\frac{\partial f}{\partial c} u_c\right)^2 + \dots} \quad (8)$$

## 3 Results and discussion

Results from the experiments are presented in form of air distribution coefficients  $d$  (%) that represent a fraction of the total airflow through the HVAC system. Each case is examined separately. Confidence level of the presented results is 95 %.

### 3.1 Summer case

An airspeed profile in the suction tube is depicted in Figure 7. Shape of the profile corresponds to an expected turbulent profile shape. It is obvious that the velocities are not evenly distributed across the tube. However, the peak ( $4.3 \text{ m s}^{-1}$ ) is caused due to the adapter shape which had to be customised to fit the inlet opening. Indication of diameters “A-B, C-D” corresponds to Figure 5.

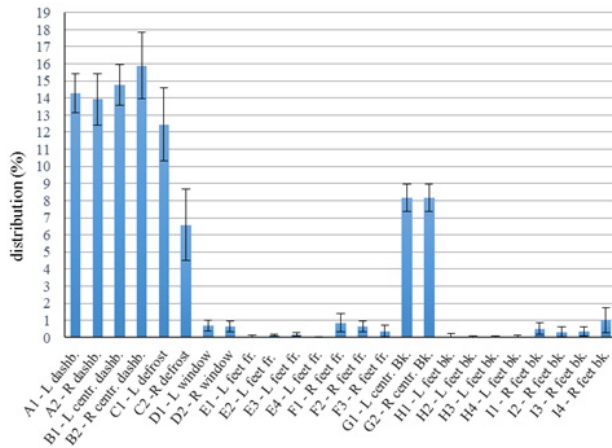


**Figure 7.** Summer case, the inlet velocity profile.

Voltage on the HVAC fan was stabilised at 4.6 V what meets approximately  $57 \text{ l s}^{-1}$  of airflow at the vents (sum of all airflows through the vents). Detailed information about the flows provides Table 4. Overall, good match of inlet and outlet airflow was achieved – the absolute difference of the mean values is  $1.6 \text{ g s}^{-1}$  ( $1 \text{ s}^{-1}$ ).

**Table 4.** Summer case, the total airflow and mass flow.

flow	inlet	outlet	difference in-out	
			absolute	relative
(g s <sup>-1</sup> )	68.6 ± 0.3	70.2 ± 3.1	1.6	2.3 %
(l s <sup>-1</sup> )	59.0 ± 0.2	57.4 ± 2.6	1.6	2.7 %

**Figure 8.** Summer case, distribution coefficients with 95% confidence error bars.

The most of the air, around 60 %, enters the cabin through dashboard vents (A1, A2, B1, B2). Next, about 20 % of the air is directed to the windshield and 16 % is conducted to the rear seats. Distribution is relatively symmetric, yet a defrost slot provided more air for the driver's section. However, relatively wide confident bars ( $\pm 2$  %) indicate either a high airspeed fluctuation or distinct measurement points. Confidence intervals of other vents range around  $\pm 1$  %. As expected, the summer setup does not provide any air to the feet compartment. Residual airflow from the “feet vents” is up to 5 % in total, and it is ascribed to the distribution door leaks.

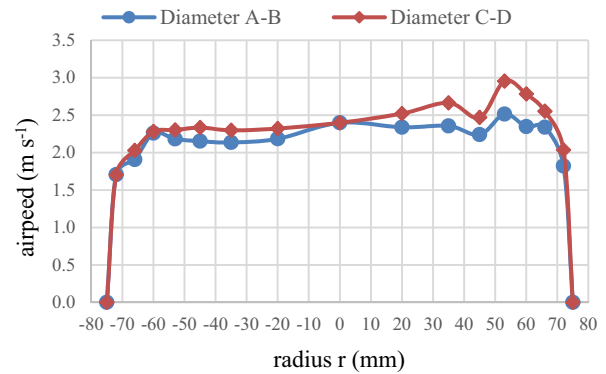
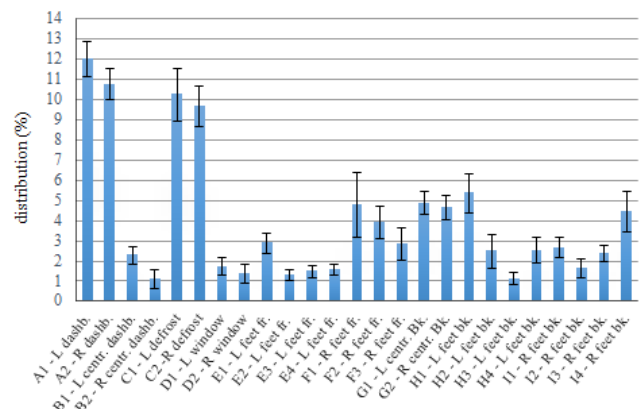
### 3.2 Spring / fall case

The airspeed profile in the suction tube is similar to the summer case one; however, the peak reaches only 3 m s<sup>-1</sup>. In average, the voltage on the fan was 3.8 V what correlates with 42 l s<sup>-1</sup> of airflow on the outlets (Table 5). That is 35 % less compared to summer case (57 l s<sup>-1</sup>). Because of the lower heat load on the cabin, lower amount of the air is necessary to treat the thermal environment.

**Table 5.** Spring / fall case, the total airflow and mass flow

flow	inlet	outlet	difference in-out	
			absolute	relative
(g s <sup>-1</sup> )	49.6 ± 0.3	49.2 ± 1.8	0.4	0.8 %
(l s <sup>-1</sup> )	40.5 ± 0.2	42.1 ± 1.6	1.6	4.0 %

According to Figure 10, distribution of the air has changed in favour of the foot well (total ca 40 %), however the distribution here is not symmetric. The dashboard vents remained opened besides the central ones (B1, B2) with about 26 % of the total airflow. Around 20 % of air was distributed towards the windows.

**Figure 9.** Spring / fall case, distribution coefficients with 95% confidence error bars.**Figure 10.** Spring / fall case, distribution coefficients with 95% confidence error bars.

### 3.3 Winter case

Theoretically, the total inlet airflow of spring / fall case and winter case should be the same because of the same voltage indicated on the HVAC fan during both experiments. Equal voltage should guarantee the same fan speed. This was assumed and the air mass flow was calculated with respect to a change of the air density with temperature (Table 6.). Although, estimated inlet airflow was used, there is 8.3% difference between the estimation and measured mass flow what is acceptable.

**Table 6.** Winter case, total flow comparison

flow	Inlet	outlet	difference in-out	
			absolute	relative
(g s <sup>-1</sup> )	52.7	48.3 ± 1.9	4.4	8.3 %
(l s <sup>-1</sup> )	40.5	40.6 ± 1.7	0.1	0.3 %

As shown in Figure 11, the air distribution is identical with the spring / fall one. However, this was expected, because majority of the air provides heating of the foot well primarily, and the rest of the air compensates radiative effect of cold windows and ensues their defogging or defrosting.



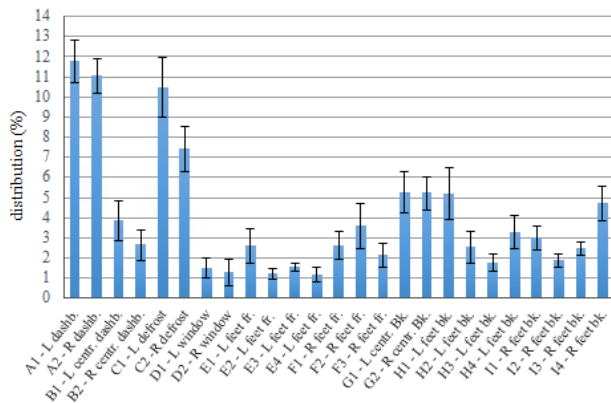


**Figure 11.** Winter case, distribution coefficients with 95% confidence error bars.

## 4 Conclusion

The aim of this study was to develop a methodology to measure airflow within a vehicle HVAC system simply and relatively precisely. Inlet and outlet HVAC airflows were studied exploiting hot wire anemometry. The test vehicle, however, remained static during the tests. The air mass flow was calculated under the prerequisite that the air is an ideal gas. Next, three climate cases were examined under steady thermal conditions. We arrived at following conclusions:

- To avoid airflow pulsations due to the cyclic opening of the air exhaust flaps, the cabin had to be connected to the ambient atmosphere (5<sup>th</sup> doors were ajar). This also means that under real driving conditions the airflow will be changed due to a rising ambient pressure with a driving speed. In the real driving conditions, this is partially solved by closing the recirculation door; however, the door was made fully opened during the tests.
- The mean values of the inlet and outlet flows match (the maximum difference is  $1.6 \text{ l s}^{-1}$  or  $4.4 \text{ g s}^{-1}$ ). Volumetric change of the air inside the HVAC unit was included in the calculations. Confidence intervals on the inlet are circa one order of magnitude smaller than on the outlet vents what is still acceptable. This could be improved, in the future, by special mounts to hold the probe precisely in its position.
- Summer case showed that the HVAC unit provides more air to compensate heat gains (ca  $57 \text{ l s}^{-1}$ ) compared to winter and spring/fall case (ca  $42 \text{ l s}^{-1}$ ).
- Air distribution in summer is focused on passengers' upper body (76 %) and windshield (20 %). Rest of the air leaks to the other vents insignificantly.
- Winter and spring / fall cases are foot well oriented (ca 40 %), the rest of the air is used to heat up the windows and improve passengers thermal comfort.
- Pair vents, besides the feet ones, provide equal amount of the air. This knowledge can be used to determine the airflow only from one vent of the pair in the future.

## References

- Office for Official Publications of the European Communities. *How Europeans spend their time*. Luxembourg: European Communities, pp. 132. ISBN 92-894-7235-9.A. (2004)
- O. David, V. Ezratty. *Energy Policy*, Vol.49, pp. 116-121. ISSN 0301-4215,(2011)
- S. Daly. *Automotive air-conditioning and climate control systems*. 1st ed. Oxford : Butterworth Heinemann. s. xvii, pp. 362. ISBN 07-506-6955-1. (2006)
- Goodfellow, H. D. and E. Tähti. *Industrial Ventilation Design Guidebook. Part 12. Experimental techniques*. (2001)
- R. Palenčár, et al., *Nejistoty v měření I: vyjadřování*. In: Automa. Brno: 7-8. pp. 50-54.(2001).
- R. Palenčár, et al., *Nejistoty v měření II: nejistoty*. In: Automa. Brno: 10. pp. 52-56.(2001).
- R. Palenčár, et al., *Nejistoty v měření III: vyjadřování*. In: Automa. Brno: 12. pp. 28-33.(2001).
- P. Němeček. *Nejistoty měření*. Praha: Česká společnost pro jakost, o.s., (2008)

## Acknowledgement

The research was supported by the project Reg. No. FSI-S-14-2355 of the Brno University of Technology; the project LO1202 Netme Centre Plus with the financial support from the Ministry of Education, Youth and Sports of the Czech Republic under the "National Sustainability Programme I" and the project of the Josef Božek Competence Centre for Automotive Industry TE01020020.